

1  
2  
3  
4  
5  
6  
7  
8  
9  
10  
11  
12  
13  
14  
15  
16  
17  
18  
19  
20  
21  
22  
23  
24  
25

**THE IMPACT OF OXY FUEL CONDITIONS ON ELEMENTAL MERCURY  
RE-EMISSION IN WFGD SYSTEMS**

Nuria Fernández-Miranda, M. Antonia Lopez-Anton\*, Teresa Torre-Santos, Mercedes  
Díaz-Somoano, M. Rosa Martínez-Tarazona

Instituto Nacional del Carbón (CSIC), Francisco Pintado Fe, 26, 33011, Oviedo, Spain

\*Corresponding author:  
Phone: +34 985 119090  
Fax: +34 985 297662  
Email: marian@incar.csic.es

26 **Abstract**

27 This study evaluates some of the variables that may influence mercury retention in wet  
28 flue gas desulfurization plants (WFGD), focusing on oxy-coal combustion processes  
29 and differences when compared with atmospheres enriched in N<sub>2</sub>. The main drawback  
30 of using WFGD for mercury capture is the possibility of unwanted reduction of  
31 dissolved Hg<sup>2+</sup>, leading to the re-emission of insoluble elemental mercury (Hg<sup>0</sup>) which  
32 decreases efficiency. To acquire a better understanding of the mercury re-emission  
33 reactions in WFGD systems, this work analyses different variables that influence the  
34 behaviour of mercury in slurries obtained from two limestones, under an oxy-  
35 combustion atmosphere. The O<sub>2</sub> supplied to the reactor, the influence of the pH, the  
36 concentration of mercury in gas phase and the enhancement of mercury in the slurry  
37 were the variables considered. The study was performed at laboratory scale where  
38 possible reactions between the components in the scrubber can be individually  
39 evaluated. It was found that in an oxy-combustion atmosphere (mostly CO<sub>2</sub>), the re-  
40 emission of Hg<sup>0</sup> is lower than under N<sub>2</sub>-enriched atmosphere and the mercury is mainly  
41 retained as Hg<sup>2+</sup> in the liquid phase.

42

43 **Keywords:** mercury; oxy-combustion; gypsum; limestone

## 44 1. Introduction

45 According to the European Environment Agency, energy production in 2013  
46 contributed more than 55% of the SO<sub>x</sub> emissions to the environment.<sup>1</sup> Control of SO<sub>x</sub>  
47 emissions in coal-fired power plants is carried out mostly by wet flue gas  
48 desulfurization systems (WFGD)<sup>2</sup> in which a variety of alkaline chemicals, though  
49 generally limestone, are used to capture the SO<sub>2</sub>.<sup>3</sup> In most WFGD scrubbing facilities,  
50 flue gas containing SO<sub>2</sub> is brought into contact with a limestone-water slurry to form  
51 insoluble calcium sulfite hemihydrate and gypsum.

52 Worth noting is that such facilities also serve as the media whereby other reactions  
53 may occur. These reactions depend on a wide variety of solid, liquid and gaseous  
54 components reaching these systems, and can be controlled and exploited to capture  
55 other undesirable constituents from the gas. The retention of oxidized species of  
56 mercury (Hg<sup>2+</sup>) in the WFGD facilities<sup>4,5</sup> is the one that has created most interest  
57 because coal-fired power plants are the main source of toxic mercury emissions.<sup>6,7</sup> A  
58 major limitation of this process is the reduction of dissolved Hg<sup>2+</sup>, leading to the re-  
59 emission of insoluble elemental mercury (Hg<sup>0</sup>) into the atmosphere and decreasing  
60 efficiency of mercury capture. To evaluate this effect, studies of mercury behavior in  
61 scrubbers have been carried out at industrial scale and conclusions have been drawn  
62 mainly by means of mass balances.<sup>3-5,8,9</sup> However, the results at industrial scale are  
63 difficult to generalize because the variables involved may not be subject to  
64 modification. This drawback can be overcome by assessing these variables in laboratory  
65 scale simulations, as possible reactions between the components in the scrubber can be  
66 individually evaluated.<sup>10,11</sup> The behavior of gaseous Hg<sup>2+</sup> when it comes into contact  
67 with a gypsum slurry has already been evaluated using a series of simple atmospheres at

68 laboratory scale,<sup>11,12</sup> the present study was carried out in typical oxy-combustion gas  
69 conditions.

70 The attraction on oxy-coal combustion is its potential to reduce CO<sub>2</sub> emissions.<sup>13,14</sup>  
71 In oxy-combustions plants, coal is burned in a mixture of O<sub>2</sub> and recirculated flue gas,  
72 resulting in a gas stream with a high concentration of CO<sub>2</sub> suitable for capture and  
73 storage (CCS). However, this technology may also produce a significant rise in SO<sub>2</sub><sup>15</sup>  
74 and mercury<sup>16</sup> concentrations (with respect to conventional air firing) as a result of the  
75 recirculation of flue gas. In oxy-combustion processes mercury species in the gas are  
76 undesirable not only because of their toxicity but also because Hg<sup>0</sup> can cause  
77 technological problems by corroding the Al-alloys in the CO<sub>2</sub> compression units.<sup>17</sup>

78 The present study is based on previous research that has demonstrated the  
79 dependence of mercury behaviour on the characteristics and composition of the  
80 limestones in WFGD conditions.<sup>2</sup> This is a consequence of the reduction of Hg<sup>2+</sup> to Hg<sup>0</sup>  
81 in the slurry caused by metals originating from the limestone impurities. In fact, a  
82 significant re-emission of Hg<sup>0</sup> in slurries obtained from limestone with a high content in  
83 Fe has been observed independently of the presence of sulphites, which may also lead to  
84 Hg<sup>0</sup> re-emission.<sup>12</sup> These findings that were obtained in an inert atmosphere represent  
85 the basic knowledge for predicting and understanding mercury behaviour in WFGD  
86 systems. However, it still needs to be confirmed in more real atmospheres.

87 As a further contribution to the interpretation and prediction of mercury behaviour  
88 in WFGD systems, the present work analyses the effect of different variables on the  
89 behaviour of mercury in slurries from two limestones under oxy-combustion conditions.  
90 The supply of O<sub>2</sub> to the reactor, the influence of the pH, the mercury concentration in

91 the gas phase and the enhancement of mercury in the slurry with time were the variables  
92 evaluated.

93

## 94 **2. Experimental**

### 95 **2.1. Limestone and slurry characterization**

96 Two limestone samples, labelled CaC and CaP, previously characterized both  
97 chemically and physically<sup>12</sup> were used to simulate SO<sub>2</sub> capture. Calcium, magnesium,  
98 aluminium, silicon, phosphorus, sodium and potassium contents were determined using  
99 a Bruker SRS3000 fluorescence spectrometer. Trace metals were analyzed by ICP-MS  
100 in a 7700X Agilent device after the samples had been digested with HNO<sub>3</sub> in a  
101 microwave oven. The species dissolved in the reactor under the experimental conditions  
102 were also determined by ICP-MS. Sulphide content in dissolution was estimated by a  
103 colorimetric method.

104 The chemical reactivity of the limestones was calculated by neutralization of a  
105 blend of 1.0 g of limestone and 1.0 g of CaSO<sub>4</sub>·2H<sub>2</sub>O with a solution of 0.5 N H<sub>2</sub>SO<sub>4</sub> at  
106 50 °C for 6 hours. The pH was kept at values of 5.0±0.1 using a Mettler Toledo DL53  
107 titrator. The limestone conversion was established as the stoichiometric ratio of  
108 sulphuric acid consumed.

### 109 **2.2. Lab-scale device**

110 The mechanisms of retention and re-emission of elemental mercury in scrubbers  
111 were simulated using the lab-scale device<sup>18</sup> described in Figure 1. The equipment  
112 consisted of i) a flue gas generation unit for obtaining oxidized mercury, ii) a glass  
113 reactor where the slurry was prepared and checked and iii) a continuous mercury

114 analyser (VM-3000) that recorded the  $\text{Hg}^0$  (mercury re-emitted) at the outlet of the  
115 reactor.

116 **Figure 1.** Experimental device used at lab scale.

117

118 A commercial gas generator system (HovaCAL GmbH) coupled to an evaporator  
119 was used to generate different concentrations of  $\text{Hg}^{2+}$  by evaporation, at 200 °C, of a  
120 mercury nitrate solution, stabilized in 10 mM of hydrochloric acid. The carrier gases  
121 used consisted of 70% of  $\text{CO}_2$  and different concentrations of  $\text{O}_2$  (4 and 20%), balanced  
122 with  $\text{N}_2$ , set to a flow rate of 3  $\text{L}\cdot\text{min}^{-1}$ . Sulphur dioxide (1000 ppm) was also included in  
123 the flow gas in specific experiments. The gas was conducted to the reactor through PFA  
124 pipes kept at temperature of 120 °C to avoid the condensation of moisture and mercury.

125 The reactor consisted of a 500 mL, three-necked, round-bottomed glass flask fitted  
126 with an inlet and an outlet for the flue gas, and an additional connection for the pH  
127 electrode and a titrator. A thermostat system supplied with a stirring unit ensured a  
128 constant temperature (40 °C) and the right mixture of mercury and slurry. The gypsum  
129 slurry was prepared by adding sulphuric acid to a limestone slurry with a 1% solid  
130 content. The pH was continuously recorded on an Orion Meter (Model 720A+) fitted  
131 with an Orion electrode 9678BNWP. When necessary, the pH was adjusted by adding  
132 1N of NaOH using a Mettler Toledo DL53 titrator.

### 133 **2.3. Mercury analysis**

134 The mercury concentration in the solid and liquid products was analysed using a  
135 LECO Automatic Mercury Analyser, AMA 254. The mercury species in the gypsum  
136 were identified by a thermal programmed desorption procedure ( $\text{HgTPD}$ )<sup>19</sup> using a  
137 continuous mercury analyzer (RA-915) coupled to a furnace (PYRO-915), both from

138 Lumex. The furnace consisted of two chambers in series, the first chamber serving to  
139 pyrolyze the solid samples and the second chamber to reduce the mercury compounds to  
140 elemental mercury. The mercury species were characterized according to the  
141 temperature range in which they were released from the sample.<sup>19</sup>

### 142 **3. Results and discussion**

143 The study was performed at laboratory scale using two limestone samples to react  
144 with SO<sub>2</sub> in two gas compositions: i) 70% CO<sub>2</sub> + 20 O<sub>2</sub>% + 10% H<sub>2</sub>O and ii) 70% CO<sub>2</sub>  
145 + 4% O<sub>2</sub> + 10% H<sub>2</sub>O + 16% N<sub>2</sub>. In each case, the distribution of mercury in the by-  
146 products produced in the reactor was compared under three different conditions:

147 (a) Precipitating the gypsum at the beginning of the experiment with sulfuric acid  
148 resulting in a pH of 5.5. Henceforth this will be referred to as conditions A (with  
149 20% O<sub>2</sub>) and A\*(with 4% O<sub>2</sub>).

150 (b) Bubbling SO<sub>2</sub> in the solution while the pH was adjusted to 5.5 by adding NaOH.  
151 Henceforth this will be referred to as conditions B (with 20% O<sub>2</sub>).

152 (c) Bubbling SO<sub>2</sub> in the slurry, which caused a decrease in the pH of the slurry  
153 during the experiments. Henceforth this will be referred to as conditions C (with  
154 20% O<sub>2</sub>).

#### 155 **3.1. Characterization of the limestones and aqueous phase**

156 The most important characteristics of limestones CaC and CaP<sup>12</sup> and the aqueous  
157 phases of the gypsum slurries designated as CaC(aq) and CaP(aq) are shown in Table 1.  
158 The average particle size and apparent porosity are of the same order in both cases, 32  
159 and 26 μm and 38 and 41% for CaC and CaP, respectively. The Ca content was ~ 39%  
160 in both limestone samples, although minor components were present in different  
161 concentrations, the most noticeable differences between CaC and CaP are the Fe (877

162  $\mu\text{g}\cdot\text{g}^{-1}$ ), Mn ( $177 \mu\text{g}\cdot\text{g}^{-1}$ ), Mg (0.27%) and Si (0.94%) contents which were higher in  
163 CaC, whereas Sr content ( $1958 \mu\text{g}\cdot\text{g}^{-1}$ ) was higher in CaP.

164 **Table 1.** Chemical composition of the liquid fraction of the slurries from CaC and CaP  
165 limestone samples.

166

167 The chemical composition of CaC(aq) and CaP(aq) (Table 1) indicates that the  
168 dissolution of elements may depend on the gas composition entering the reactor, which  
169 in turn might modify the pH of the slurry. Three main significant remarks need to be  
170 made concerning the data in Table 1:

171 i) There is no correlation between the concentration of impurities dissolved and its  
172 content in the limestone.

173 ii) The composition of the inlet flue gas affects the dissolution of some impurities,  
174 especially in the slurry from CaP. When  $\text{O}_2$  increased from 4% to 20% the dissolution  
175 of elements such as Mg, Mn, Ni, Fe and Zn slightly decreased probably as consequence  
176 of pH and Eh variations. While the pH remains nearly constant at conditions A with  
177 CaC slurry, in the case of CaP is more acid at the beginning of the experiments.

178 iii) A great increase in acidity in the medium, as occurred in conditions C, where  
179 the pH values decreased from 5.5 to 1.8, favors the dissolution of some metals. A  
180 portion of sulfur species in solution cannot be ruled out in these conditions.

181

### 182 **3.2. Effect of oxygen supply on Hg behaviour**

183 WFGD can operate under natural or under forced oxidation conditions where  $\text{O}_2$  is  
184 injected into the tank to ensure full oxidation of the sulphur by-products.<sup>20</sup> To evaluate



185 the effect of increasing O<sub>2</sub> on mercury re-emission, inlet flue gases containing 150  
186 μg·m<sup>-3</sup> of Hg<sup>2+</sup> and different concentrations of O<sub>2</sub> were bubbled into the slurries  
187 prepared with CaC and CaP limestones. The percentages of CO<sub>2</sub> and water vapour in  
188 the inlet gas stream were kept constant at 70% and 10%, respectively. In these  
189 conditions, the pH of the slurries reaches a value of 5.5 during most of the experiment  
190 (Conditions A and A\*). For both concentrations of O<sub>2</sub> (4 and 20%), the re-emitted Hg<sup>0</sup>  
191 was less than 13% of the inlet Hg<sup>2+</sup>, remaining almost constant during the test (Figure  
192 2). The increase in the O<sub>2</sub> concentration caused a slight drop (approximately 3%), in the  
193 re-emission of Hg<sup>0</sup> in the slurries. This is consistent with results of a previous study<sup>21</sup>  
194 which concluded that O<sub>2</sub> content in the inlet flue gas higher than 5% stabilizes Hg<sup>2+</sup> in  
195 the slurry.

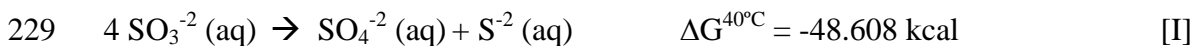
196 **Figure 2.** Partitioning of Hg in the gas, liquid and solid by-products of the scrubber  
197 from CaC and CaP limestones. Flue gas composition: 70% CO<sub>2</sub> + 10% H<sub>2</sub>O + O<sub>2</sub> (4 or  
198 20%) + N<sub>2</sub> (balance) + 150 μg·m<sup>-3</sup> Hg.  
199

200 Figure 2 illustrates the partitioning of mercury in the by-products. Apart from the  
201 amount of Hg<sup>0</sup> re-emitted, the distribution of mercury between the liquid and solid  
202 differed considerably in the two slurries. Most of the mercury was dissolved in the  
203 aqueous phase in both slurries, but in the case of CaP slurry the concentration of  
204 mercury was higher in the solid fraction. The S<sup>2-</sup> content in the liquid phase of the CaP  
205 slurry was analysed but the detection limit (0.1 mg/L) for this species was not reached.  
206 Although the dissolution of soluble sulphides potentially present in CaP limestone could  
207 not be proven, the formation of HgS from S<sup>2-</sup>-dissolved should not be ruled out. The  
208 mercury species present in the solid fraction of CaP were identified by HgTPD (Figure  
209 3).

210 **Figure 3.** Mercury thermal decomposition profile of gypsum from CaP limestone. Flue  
211 gas composition: 70% CO<sub>2</sub> + 10% H<sub>2</sub>O + 4% O<sub>2</sub> + 16% N<sub>2</sub> + 150 μg·m<sup>-3</sup> Hg.  
212

213 The desorption profiles show two peaks, the main one at around 190±11 °C and a  
214 second one, of less intensity, at 305±12 °C. According to a previous study carried out  
215 using the HgTPD technique<sup>22</sup>, these temperatures correspond to desorption of black  
216 HgS and red HgS, respectively. Although red HgS is more stable than black HgS,  
217 systems with favorable thermodynamic conditions may produce black HgS. In fact,  
218 previous studies have identified these species in gypsum samples from scrubbers<sup>22,23</sup>.  
219 However, the exact mechanisms involved in the formation of HgS have not yet been  
220 established.

221 Some mechanisms have been suggested in the literature<sup>24,25</sup> to explain the  
222 formation of HgS. Although they cannot be ratified from the results of this work, cannot  
223 be discarded. When discussing these possible mechanisms, it must be borne in mind that  
224 the reaction of SO<sub>2</sub>(g) with limestone produces CaSO<sub>3</sub> which, in the presence of O<sub>2</sub>,  
225 forms CaSO<sub>4</sub>. Although sulfide is not normally present in WFGD slurries and sulfites  
226 are not stable at pH values lower than 6, the following mechanism is suggested whereby  
227 mercury might catalyze the disproportionation of sulfite<sup>24</sup> to yield sulfate and sulfide  
228 (reaction I).



230 There is some preliminary spectrophotometric evidence<sup>24</sup> to suggest that mercury  
231 catalyzes the reduction of sulfites even when this reaction is thermodynamically favored  
232 but very slowly under most conditions. This means that sulfide would be close to

233 mercury at a molecular level and it could then react to form insoluble HgS<sup>24</sup> according  
234 to reaction II.



236 This interpretation would explain the formation of HgS in the slurries identified by  
237 HgTPD (Figure 3). Moreover, the formation of HgS depends on O<sub>2</sub> concentration. As  
238 can be observed in Figure 2, the precipitation of HgS was slightly lower in the  
239 atmosphere richest in O<sub>2</sub>. According to reaction III, an increase of O<sub>2</sub> content would  
240 produce less sulfite and consequently less sulphide (reaction I).



242 To the best of our knowledge, this mechanism has still not been confirmed, but in  
243 any case, it is not the only possible mechanism responsible for the formation of HgS.  
244 The presence of CO(g) in the gas would act as reducing agent for SO<sub>4</sub><sup>2-</sup> (reaction IV), as  
245 has been previously postulated<sup>25</sup>, generating sulfides that would immediately react with  
246 Hg<sup>+2</sup> to precipitate mercury as HgS. However in our particular case we have not  
247 identified CO(g) in the gas atmosphere in significant amounts.



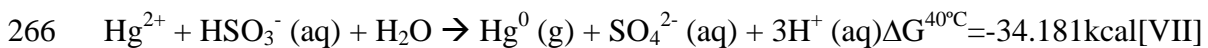
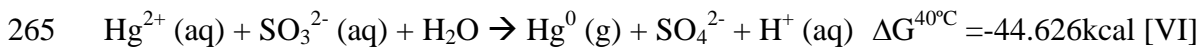
249 In any case, the concentration of HgS is considerably higher in the gypsum  
250 obtained from CaP than in the gypsum from CaC (Figure 2). This could be a  
251 consequence of the presence of a higher content of Fe impurities in CaC (Table 1) that  
252 would favor the formation of FeS instead of HgS due to the competitive reaction V.



254 Furthermore, the lower reactivity observed in CaP than CaC would involve a higher  
255 concentration of available  $\text{SO}_3^{2-}$  and  $\text{HSO}_3^{2-}$  species which could be reduced to form  
256  $\text{HgS}$ , as previously explained (reactions I and II).

### 257 **3.3. Influence of the pH on mercury re-emission under oxy-fuel conditions.**

258 Figure 4 shows the distribution of mercury when tests were performed by  
259 precipitating the limestones under conditions A, B and C. In the experiments where  $\text{SO}_2$   
260 was bubbled through the slurries (condition C),  $\text{Hg}^0$  re-emission was maximum ~30%  
261 for CaC and ~50% for CaP, as a consequence of the fall in pH. If, as is widely accepted,  
262 variations in the pH of the scrubber liqueur determine the presence of reductive species,  
263 thereby modifying  $\text{Hg}^0$  re-emission<sup>26,27</sup>, the mechanisms that might explain this  
264 behaviour are summarized in reactions VI and VII.



267 **Figure 4.** Partitioning of Hg in the gas, liquid and solid by-products of the scrubber  
268 from CaC and CaP limestones under conditions A, B and C.

269

270 The role of sulfites has been questioned in some conditions. Some studies have  
271 demonstrated that when sulfites are present in high concentrations they may form  
272 complexes with  $\text{Hg}^{2+}$ , stabilizing these species in the liquid<sup>10,11</sup>. Moreover, some studies  
273 have reported that at least in conditions A and B no sulfites were present<sup>21</sup>. If sulfites  
274 were not the factor responsible for  $\text{Hg}^{2+}$  reduction, other species in the slurry may have  
275 reduced  $\text{Hg}^{2+}$  to  $\text{Hg}^0$ . The mechanisms proposed involve reactions with specific metals,  
276 especially Fe, according to reaction VIII.



278 In fact, when different concentrations of Mn (<sup>2+</sup> and <sup>4+</sup>), Ni (<sup>2+</sup> and <sup>3+</sup>), and Fe (<sup>2+</sup>  
279 and <sup>3+</sup>) were introduced to the slurry from CaC limestone, only in the case of Fe<sup>2+</sup> the  
280 re-emission of Hg<sup>0</sup> was observed.

281 When the re-emission of Hg<sup>0</sup> under conditions A, B and C is compared (Figure 4),  
282 differences are observed. It must be remembered that B and C were performed by  
283 bubbling SO<sub>2</sub> into the limestone slurry, but B maintaining a constant pH (5.5), and C  
284 varying as consequence of the dissolution of SO<sub>2</sub>. It is observed that Hg<sup>0</sup> re-emission  
285 decreased at pH 5,5. This re-emission is nearby to the obtained in condition A, where  
286 gypsum was precipitated before that mercury species had reached the reactor. Figure 4  
287 also shows that the formation of HgS was higher in the gypsum produced under  
288 conditions B, following reactions I, II, or IV ,

289

### 290 **3.4. Effect of mercury concentration in gas phase**

291 As already mentioned, the partial recirculation of flue gases in an oxy-combustion  
292 power plant enhances the concentration of mercury in the gas entering the WFGD over  
293 time<sup>18</sup>. This is apart from the fact that the proportion of Hg<sup>2+</sup> and Hg<sup>0</sup> in the scrubber  
294 may vary in each power plant, because mercury in the flue gas not only depends on coal  
295 characteristics but also on the performance of the SCR (Selective Catalytic Reduction)  
296 in the NOx reduction<sup>28</sup> and the particle capture systems.<sup>29</sup>

297 Experiments designed to determine the influence of Hg concentration in the gas  
298 were performed using slurries prepared with the gypsum precipitated with H<sub>2</sub>SO<sub>4</sub>  
299 (condition A). The gas streams contained 25, 50 and 150 μg·m<sup>-3</sup> of Hg<sup>2+</sup>. In all cases the  
300 re-emission of Hg<sup>0</sup> was lower than 13%. In contrast to previous results performed in

301 other atmospheres<sup>10</sup>, the re-emission of  $\text{Hg}^0$  was not a function of the mercury  
302 concentration in the inlet gas, probably due to the high  $\text{O}_2$  content (20%) present in the  
303 oxy-combustion atmosphere used in this study (section 2.2). However, the partitioning  
304 of mercury in the by-products differed significantly. Figure 5 shows the different  
305 mercury contents in gypsum and water and re-emitted in the gas from the slurries CaC  
306 and CaP when the experiment was performed under conditions A (pH 5.5). Three  
307 important conclusions can be drawn:

- 308 i) In both gypsum slurries the re-emission of  $\text{Hg}^0$  is low and of the same order,  
309 regardless of the concentration of  $\text{Hg}^{2+}$  reaching the slurry.
- 310 ii) The quantity of  $\text{Hg}^{2+}$  retained in the water increases with the increase in the  
311 concentration of mercury entering the slurry.
- 312 iii) As previously observed (Figure 4), the quantity of  $\text{Hg}^{2+}$  retained in the gypsum  
313 depends on the characteristics of the slurry. When CaC limestone was used to  
314 precipitate gypsum,  $\text{Hg}^{2+}$  was preferentially retained in the water, whereas when  
315 CaP limestone was used a significant amount of  $\text{Hg}^{2+}$  remained in the gypsum as  
316  $\text{HgS}$ . Moreover, as the  $\text{Hg}^{2+}$  concentration in the gas increased, the mercury  
317 content in the gypsum obtained from CaP increased while it remained constant  
318 in the gypsum formed from CaC (Figure 5).

319

320 **Figure 5.** Hg content in the gas, liquid and solid by-products of the scrubber from CaC  
321 and CaP limestones at different Hg concentrations in gas phase. Flue gas composition:  
322 70%  $\text{CO}_2$  + 10%  $\text{H}_2\text{O}$  + 20%  $\text{O}_2$ .

323

324 **3.5. Effect of mercury accumulation in the reactor**

325 The water used in most WFGD systems is a blend of fresh and recycled water, a  
326 portion of which has gone through a filtration process for the separation of gypsum.  
327 Consequently, the water blend employed in industrial scrubbers to prepare the limestone  
328 slurry is being continuously enriched with the dissolved species in the scrubber.<sup>30</sup> Since  
329 the  $\text{Hg}^{2+}$  content in the water increases, the chemical and physical interactions  
330 responsible for the re-emission of  $\text{Hg}^0$  and the partitioning of mercury between the solid  
331 and liquid phases may change. To evaluate this effect experiments were performed  
332 under conditions A (using  $\text{H}_2\text{SO}_4$  as precipitating agent) and C (bubbling  $\text{SO}_2$ ). They  
333 were performed for CaC and CaP slurries to which 1, 2 and 5  $\text{mg}\cdot\text{L}^{-1}$  of  $\text{Hg}^{2+}$ , were  
334 added to simulate recycled water.

335 **Figure 6.** Partitioning of Hg and pH values in the slurry from CaC limestone under a)  
336 condition C (bubbling  $\text{SO}_2$ ) and b) condition A (precipitating gypsum with  $\text{H}_2\text{SO}_4$ ). Flue  
337 gas composition: 70%  $\text{CO}_2$  + 10%  $\text{H}_2\text{O}$  + 20%  $\text{O}_2$  + 150  $\mu\text{g}\cdot\text{m}^{-3}$  Hg.

338

339 The partitioning of mercury in both slurries exhibited the same trend. Figure 6  
340 shows the results for the slurry from CaC limestone. The results showed that in both  
341 conditions, A and C, the re-emission of  $\text{Hg}^0$  was higher than when fresh water was used  
342 to prepare the slurry. Moreover, the re-emission increased as the  $\text{Hg}^{2+}$  concentration in  
343 the recycled water increased.

344 The behavior of mercury in experiments performed under conditions C was more  
345 noticeable (Figure 6). As was previously explained (section 3.3) a decrease in the pH  
346 values produces an increase of mercury re-emission.

347

348 **4. Final remarks: the influence of  $\text{CO}_2$  and  $\text{O}_2$  on mercury re-emission**

349 Since the final objective of this study was to determine the effect of oxy-  
350 combustion conditions on the behavior of mercury in a scrubber at laboratory scale, the  
351 results obtained in the atmospheres with  $150 \mu\text{g}\cdot\text{m}^{-3}$  Hg, 70%  $\text{CO}_2$ , 10%  $\text{H}_2\text{O}$  and (4-  
352 20%)  $\text{O}_2$ , will now be compared with those obtained previously under  $\text{N}_2$ -enriched  
353 atmospheres using the same limestones.<sup>11,12,18</sup>

354 In the  $\text{N}_2$  atmosphere (pH 7),<sup>12</sup> the re-emission of  $\text{Hg}^0$  was nearly 100% according  
355 to the evaluation of the slurry from CaC limestone, whereas in the case of CaP slurry  
356 almost 100% of the  $\text{Hg}^{2+}$  was retained in the gypsum. Stabilization of the pH in the  $\text{CO}_2$   
357 atmosphere (pH 5.5) with different concentrations of  $\text{O}_2$  prevented the reduction  
358 reactions. The lower mercury re-emission observed in oxy-combustion atmosphere  
359 confirms previous observations<sup>21</sup> and the same effect ought to occur in all limestones of  
360 similar characteristics to CaC.

361 If the pH decreases ( $< 5.5$ ), as occurred in experiments performed under conditions  
362 C, the re-emission will increase regardless of  $\text{O}_2$  concentration. However, if the pH is  
363 stable (condition A), an increase in the  $\text{O}_2$  concentration will cause a drop in the re-  
364 emission of  $\text{Hg}^0$  in the slurries because  $\text{O}_2$  is involved in the reduction reactions.

365 There is a parallel behavior between re-emission and characteristics of the slurry  
366 whatever the atmosphere. Under oxy-combustion and  $\text{N}_2$  conditions,<sup>12</sup> the mercury  
367 captured in the solid phase as  $\text{HgS}$  was always higher in CaP slurry than in CaC slurry.

368

369 **Acknowledgements**



370 The financial support for this work was provided by the National Research Program  
371 under project CTM2011–22921. The authors also thank PCTI Asturias for awarding  
372 Nuria Fernandez-Miranda a pre-doctoral fellowship.

373

## 374 **References**

375

376 (1) Europe Environment Agency (EEA). European Union emission inventory report  
377 1990-2013 under the UNECE Convention on Long-range Transboundary Air  
378 Pollution (LRTAP) EEA. Technical report n° 8/2015, 2015;  
379 <http://www.eea.europa.eu/publications/lrtap-emission-inventory-report>

380 (2) United States Environmental Protection Agency (US EPA). Controlling SO<sub>2</sub>  
381 emissions: a review of technologies. EPA/600/R-00/093, 2000;  
382 <http://nepis.epa.gov/Adobe/PDF/P1007IQM.pdf>

383 (3) United States Environmental Protection Agency (US EPA). Control of mercury  
384 emissions from coal-fired electric utility boilers. EPA/600/R-01/109, 2002;  
385 <http://nepis.epa.gov/Adobe/PDF/P10071NU.PDF>

386 (4) Cheng, C-M.; Hack, P.; Chu, P.; Chang, Y-N.; Lin, T-Y.; Ko, C-S.; Chiang, P-  
387 H.; He, C-C.; Lai, Y-M.; Pan, W-P. Partitioning of mercury, arsenic, selenium,  
388 boron and chloride in a full-Scale combustion process equipped with selective  
389 catalyst reduction, electrostatic precipitation and flue gas desulfurization  
390 systems. *Energ. Fuel.* **2009**, 23, 4805-4816.

391 (5) Pavlish, J. H.; Sondreal, E. A.; Mann, M. D.; Olson, E. S.; Galbreath, K. C.;  
392 Laudal, D. L.; Benson, S. A. Status review of mercury control options for coal-  
393 fired power plants. *Fuel Process. Technol.* **2003**, 82, 89-165.

- 394 (6) Rallo, M.; López-Antón, M. A.; Contreras, M. L.; Maroto-Valer, M. M. Mercury  
395 policy and regulations for coal-fired power plants. *Environ. Sci. Pollut. R.* **2012**,  
396 *19*, 1084-1096.
- 397 (7) United Nations Environment Programme (UNEP). Global Mercury Assessment  
398 2013: Sources, Emissions, Releases and Environmental Transport. UNEP  
399 Chemicals Branch, 2013;  
400 <http://www.unep.org/PDF/PressReleases/GlobalMercuryAssessment2013.pdf>
- 401 (8) Ochoa-González, R.; Córdoba, P.; Díaz-Somoano, M.; Font, O.; López-Antón,  
402 M. A.; Leiva, C.; Martínez-Tarazona, M. R.; Querol, X.; Pereira, C. F.; Tomás,  
403 A.; Gómez, P.; Mesado, P. Differential partitioning and speciation of Hg in wet  
404 FGD facilities of two Spanish PCC power plants. *Chemosphere* **2011**, *85* (4),  
405 565-570.
- 406 (9) Wu, C. L.; Cao, Y.; Li, H. X.; Pan, W. P. Full scale evaluation and suppression  
407 of mercury re-emission in wet flue gas desulfurization system. *Applied*  
408 *Mechanics and Materials* **2013**, *316-317*, 354-357.
- 409 (10) Omine, N.; Romero, C. E.; Kikkawa, H.; Wu, S.; Eswaran, S. Study of elemental  
410 mercury re-emission in a simulated wet scrubber. *Fuel* **2012**, *91*, 93-101.
- 411 (11) Ochoa-González, R.; Díaz-Somoano, M.; Martínez-Tarazona, M. R. The capture  
412 of oxidized mercury from simulated desulphurization aqueous solutions. *J.*  
413 *Environ. Manage.* **2013**, *120*, 55-60.
- 414 (12) Ochoa-González, R.; Díaz-Somoano, M.; Martínez-Tarazona, M. R. Influence of  
415 limestone characteristics on mercury re-emission in WFGD systems. *Environ.*  
416 *Sci. Technol.* **2013**, *47*, 2974-2981.

- 417 (13) Scheffknecht, G.; Al-Makhadmeh, L.; Schnell, U.; Maier, J. Oxy-fuel coal  
418 combustion - A review of the current state-of-the-art. *Int. J. Greenh. Gas Cont.*  
419 **2011**, *5*, S16-S35.
- 420 (14) Stanger, R.; Wall, T.; Spörl, R.; Paneru, M.; Grathwohl, S.; Weidmann, M.;  
421 Scheffknecht, G.; McDonald, D.; Myöhänen, K.; Ritvanen, J.; Rahiala, S.;  
422 Hyppänen, T.; Mletzko, J.; Kather, A.; Santos, S. Oxyfuel combustion for CO<sub>2</sub>  
423 capture in power plants. *Int. J. Greenh. Gas Con.* **2015**, *40*, 55-125.
- 424 (15) Wall, T. F. Combustion processes for carbon capture. *Proceeding of the*  
425 *Combustion Institute.* **2007**, *31*, 31-47.
- 426 (16) Roy, B.; Choo, W. L.; Bhattacharya, S. Prediction of distribution of trace  
427 elements under oxy-fuel combustion conditions using Victoria brown coals. *Fuel*  
428 **2013**, *114*, 135-142.
- 429 (17) Bessone, J. B. The activation of aluminium by mercury ions in non-aggressive  
430 media. *Corros. Sci.* **2006**, *48*, 4243-4256.
- 431 (18) Ochoa-Gonzalez, R.; Díaz-Somoano, M.; Martínez-Tarazona, M. R. Effect of  
432 anion concentrations on Hg<sup>2+</sup> reduction from simulated desulphurization  
433 aqueous solutions. *Chem. Eng. J.* **2013**, *214*, 165-171.
- 434 (19) Rumayor, M.; Díaz-Somoano, M.; Lopez-Anton, M. A.; Martinez-Tarazona, M.  
435 R. Mercury compounds characterization by thermal desorption. *Talanta* **2013**,  
436 *114*, 318-322.
- 437 (20) Reference document on best available techniques for large combustion plants,  
438 (BREFs). 2006. <http://eippcb.jrc.ec.europa.eu/reference/>
- 439 (21) Ochoa-González, R.; Díaz-Somoano, M.; Martínez-Tarazona, M. R. A  
440 comprehensive evaluation of the influence of air combustion and oxy-fuel

- 441 combustion flue gas constituents on Hg<sub>0</sub> re-emission in WFGD systems. *J.*  
442 *Hazard. Mater.* **2014**, *276*, 157-163.
- 443 (22) Rumayor, M.; Díaz-Somoano, M.; López-Antón, M. A.; Ochoa-Gonzalez, R.;  
444 Martinez-Tarazona, M. R. Temperature programmed desorption as a tool for the  
445 identification of mercury in wet-desulphurization systems. *Fuel* **2015**, *148*, 98-  
446 103.
- 447 (23) Rallo M.; López-Antón M. A.; Perry R.; Maroto-Valer M. M. Mercury  
448 speciation in gypsums produced from flue gas desulfurization by temperature  
449 programmed decomposition. *Fuel* **2010**, *89*, 2157-2159.
- 450 (24) United States National Energy Technology Laboratory and EPRI. Bench-scale  
451 kinetics study of mercury reactions in FDG liquors. Technical Report DE-FC26-  
452 04NT42314, 2008.
- 453 (25) Cordoba, P.; Maroto-Valer, M. M.; Ayora, C.; Perry, R.; Rallo, M.; Font, O.;  
454 Izquierdo, M.; Querol, X. Unusual speciation and retention of Hg at a coal-fired  
455 power plant. *Environ. Sci. Technol.* **2012**, *46*, 7890-7897.
- 456 (26) Chen, C.; Zhang, J. The effect of anions on mercury re-emission from wet flue  
457 gas desulfurization liquors. *Fourth International Conference on Intelligent*  
458 *Computation Technology and Automation*, Shenzhen, China, 2011.
- 459 (27) Wo, J.; Zhang, M.; Cheng, X.; Zhong, X.; Xu, X. Hg<sup>2+</sup> reduction and re-  
460 emission from simulated wet flue gas desulfurization liquors. *J. Hazard. Mater.*  
461 **2009**, *172*, 1106-1110.
- 462 (28) Fernández-Miranda, N.; Lopez-Anton, M. A.; Díaz-Somoano, M.; Martinez-  
463 Tarazona, M. R. Mercury oxidation in catalysts used for selective reduction of  
464 NO<sub>x</sub> (SCR) in oxy-fuel combustion. *Chem. Eng. J.* **2016**, *285*, 77-82.

- 465 (29) Fernández-Miranda, N.; Lopez-Anton, M. A.; Díaz-Somoano, M.; Martínez-  
466 Tarazona, M. R. Mercury retention by fly ashes from oxy-fuel processes. *Energ.*  
467 *Fuel* **2015**, 29 (4), 2227-2233.
- 468 (30) Cordoba, P.; Font, O.; Izquierdo, M.; Querol, X.; Tobías, A.; López-Antón, M.  
469 A.; Ochoa-González, R.; Díaz-Somoano, M.; Martínez-Tarazona, M. R.; Ayora,  
470 C.; Leiva, C.; Fernández, C.; Giménez, A. Enrichment of inorganic trace  
471 pollutants in recirculated water streams from wet limestone flue gas  
472 desulfurization system in two coal power plants. *Fuel Process. Technol.* **2011**,  
473 92, 1764-1775.
- 474

475 **Figure captions**

476

477 **Figure 1.** Experimental device used at lab scale.

478

479 **Figure 2.** Partitioning of Hg in the gas, liquid and solid by-products of the scrubber  
480 from CaC and CaP limestones. Flue gas composition: 70% CO<sub>2</sub> + 10% H<sub>2</sub>O + O<sub>2</sub> (4 or  
481 20%) + N<sub>2</sub> (balance) + 150 µg·m<sup>-3</sup> Hg.

482

483 **Figure 3.** Mercury thermal decomposition profile of gypsum from CaP limestone. Flue  
484 gas composition: 70% CO<sub>2</sub> + 10% H<sub>2</sub>O + 4% O<sub>2</sub> + 16% N<sub>2</sub> + 150 µg·m<sup>-3</sup> Hg.

485

486 **Figure 4.** Partitioning of Hg in the gas, liquid and solid by-products of the scrubber  
487 from CaC and CaP limestones under conditions A, B and C.

488

489 **Figure 5.** Hg content in the gas, liquid and solid by-products of the scrubber from CaC  
490 and CaP limestones at different Hg concentrations in gas phase. Flue gas composition:  
491 70% CO<sub>2</sub> + 10% H<sub>2</sub>O + 20% O<sub>2</sub>.

492

493 **Figure 6.** Partitioning of Hg and pH values in the slurry from CaC limestone under a)  
494 condition C (bubbling SO<sub>2</sub>) and b) condition A (precipitating gypsum with H<sub>2</sub>SO<sub>4</sub>). Flue  
495 gas composition: 70% CO<sub>2</sub> + 10% H<sub>2</sub>O + 20% O<sub>2</sub> + 150 µg·m<sup>-3</sup> Hg.

496

**Table 1.** Chemical composition of the liquid fraction of the slurries from CaC and CaP limestone samples.

	CaC <sup>12</sup>	CaC(aq)			CaP <sup>12</sup>	CaP(aq)		
		Conditions A* (4%O <sub>2</sub> + H <sub>2</sub> SO <sub>4</sub> )	Conditions A (20%O <sub>2</sub> + H <sub>2</sub> SO <sub>4</sub> )	Conditions C (20%O <sub>2</sub> + SO <sub>2</sub> )		Conditions A* (4%O <sub>2</sub> + H <sub>2</sub> SO <sub>4</sub> )	Conditions A (20%O <sub>2</sub> + H <sub>2</sub> SO <sub>4</sub> )	Conditions C (20%O <sub>2</sub> + SO <sub>2</sub> )
Ca (ppm)	39.1	406	407	391	39.2	420	384	279
K (ppm)	<100	75	308	315	<100	100	174	131
Mg (ppm)	2700	13	14	21	1800	9.0	6,8	8,7
Na (ppm)	<100	1,7	2,2	5.2	<100	2,7	2,6	4,3
Mn (ppm)	177	0.7	0.7	1.0	53	2.8	2.2	2.2
Sr (ppm)	211	0.6	0.6	1.0	1958	2.1	1.8	1.9
Fe (ppm)	877	0.17	0.23	1,6	90	0.5	0.11	2,5
P (ppm)	<100	0.003	N.D.	1.2	<100	0.002	N.D.	1.0
S (ppm)	N.D	N.D.	0.01	126	300	N.D.	N.D.	80
Si (ppb)	9400	5	N.D.	253	7300	4	N.D.	760
Zn (ppb)	7.0	2	3	24	6.4	11	3	67
Al (ppb)	900	N.D.	N.D.	38	900	8	N.D.	149
Cr (ppb)	<100	N.D.	N.D.	3	<100	N.D.	N.D.	
Co (ppb)	500	N.D.	N.D.	N.D.	300	18	14	15
Ni (ppb)	<100	2	2	6	<100	11	8	16
Cu (ppb)	1200	N.D.	N.D.	16	1100	N.D.	N.D.	45
Pb (ppb)	400	<1	<1	17	500	<1	<1	30
As (ppb)	600	N.D.	N.D.	2	500	N.D.	N.D.	4
Sn (ppb)	<100	N.D.	N.D.	5	<100	N.D.	N.D.	3
Sb (ppb)	<100	3	N.D.	6	<100	N.D.	N.D.	2

**N.D.:** not detected



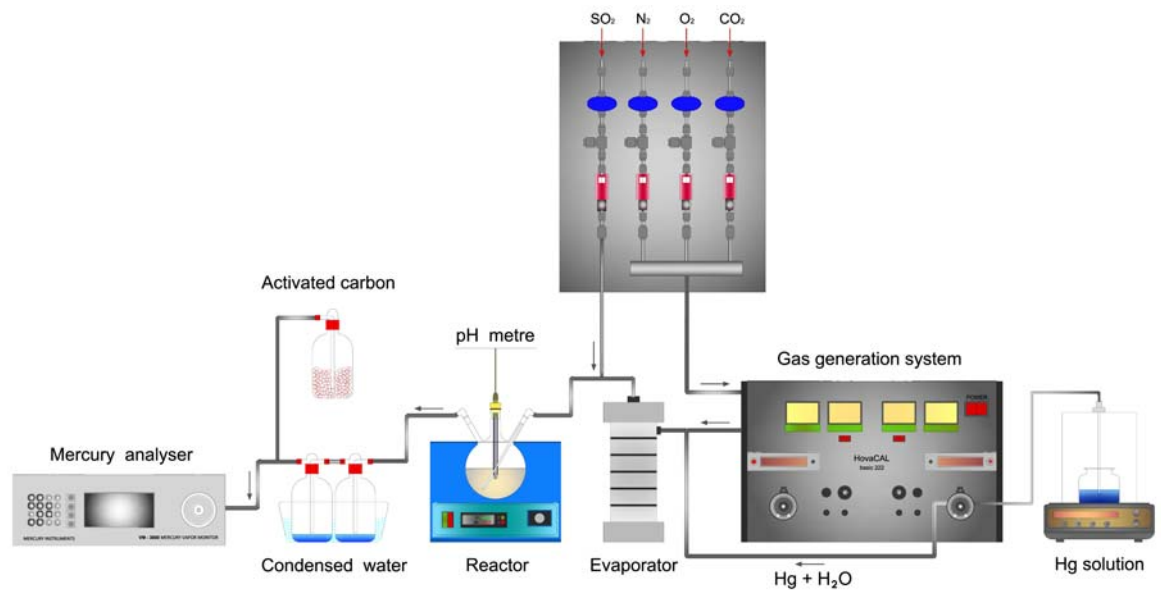


Figure 1

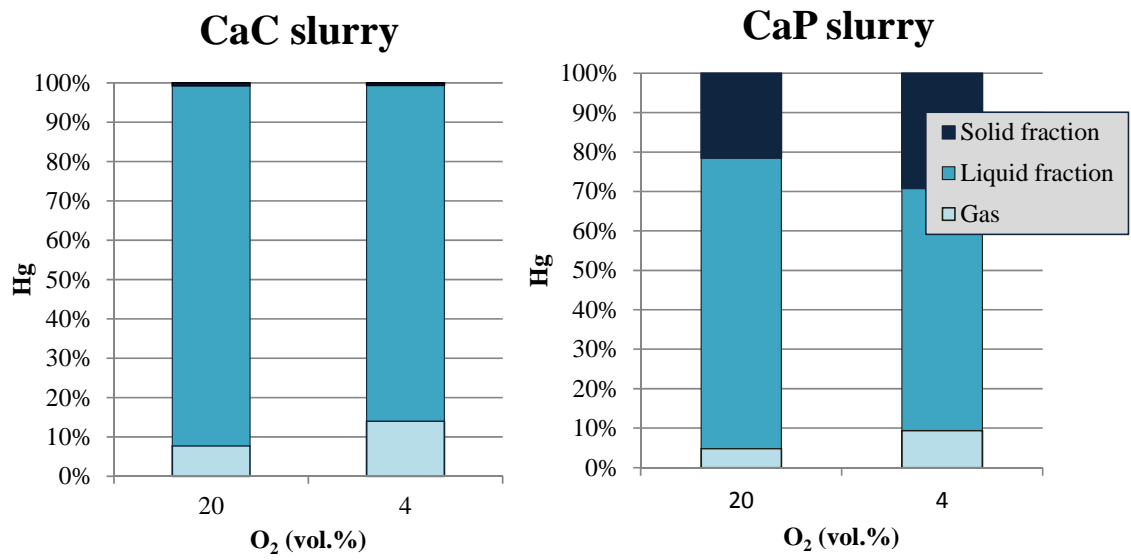


Figure 2

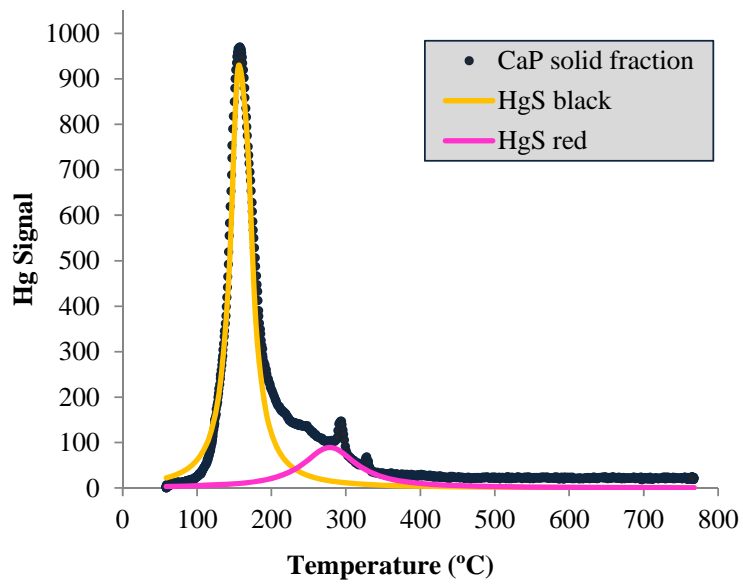


Figure 3

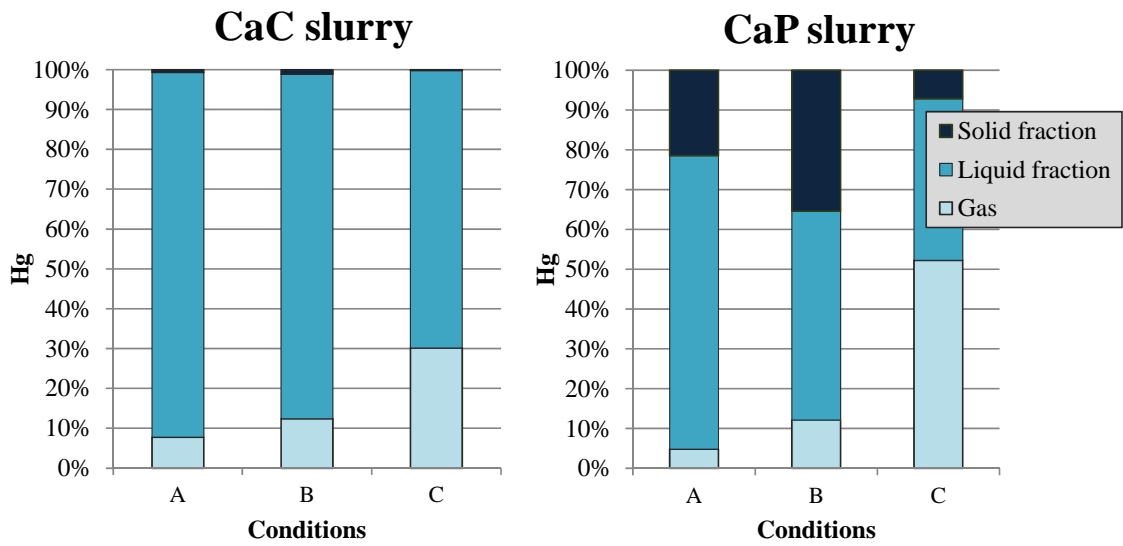


Figure 4

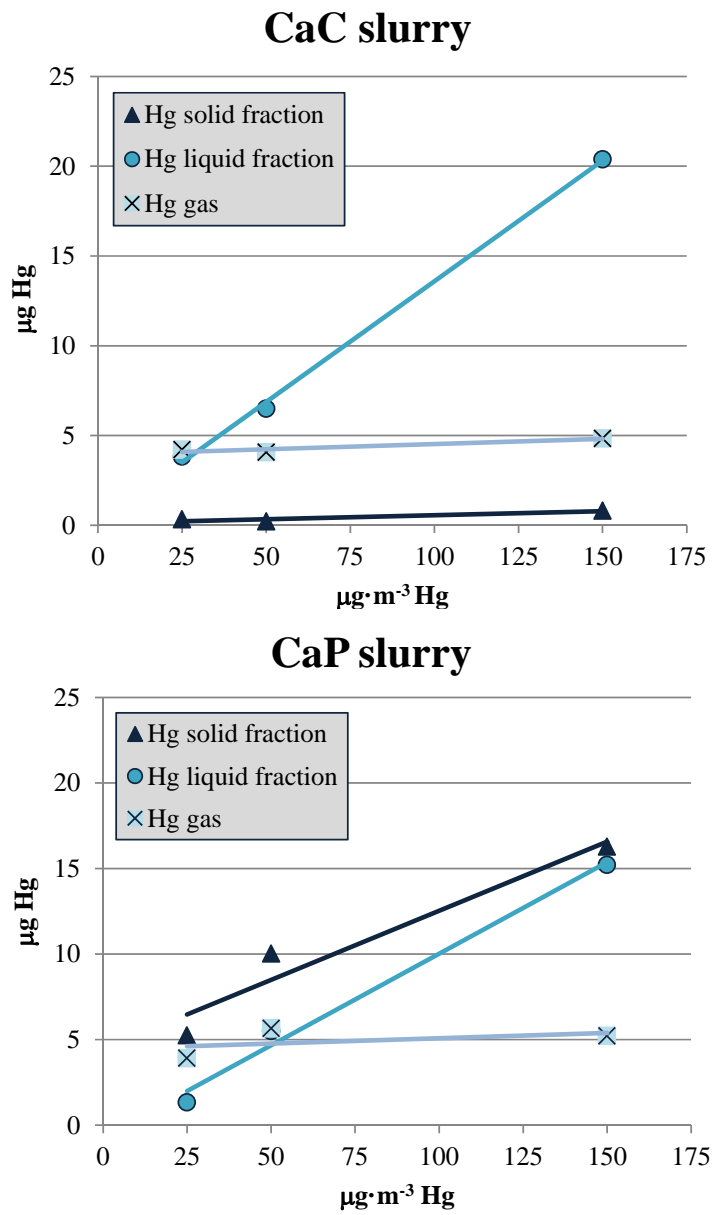
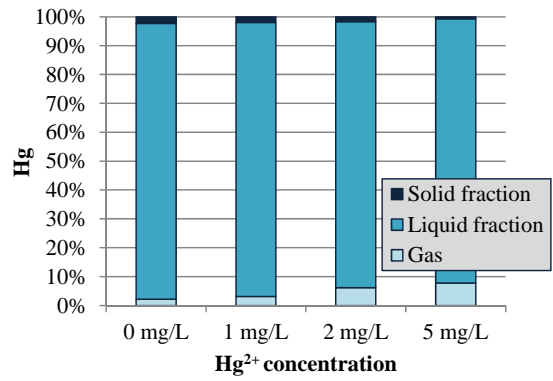
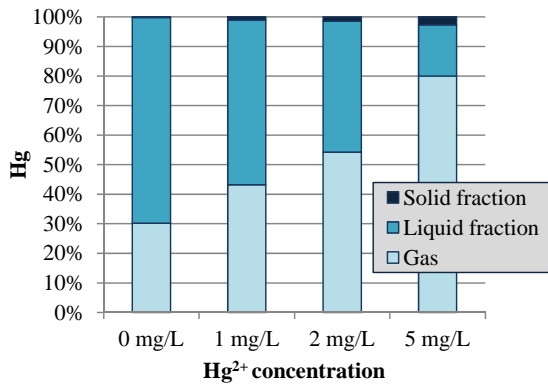
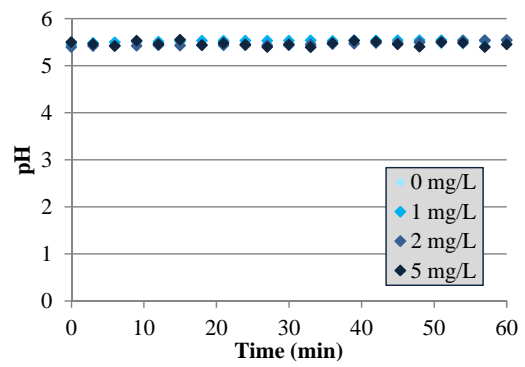
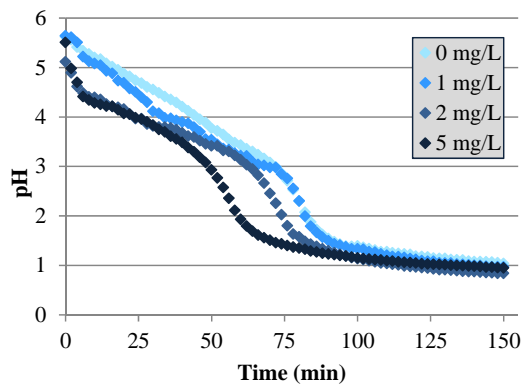


Figure 5



(a)

(b)

Figure 6